

Performance Evaluation of (MIG) And Tungsten Inert Gas (TIG) Welding Using Simufact Approach.

¹I.I. Okachi, ²E.O. Isaac, ³A.N. Thomas, ⁴Tasie Martins Chizi

^{1, 2, 3, 4} Department of Mechanical Engineering, Rivers State University, Port Harcourt, Rivers State, Nigeria.

Corresponding Author: ikegwuru.okachi@ust.edu.ng

ABSTRACT: This study evaluates performance of Metal Inert Gas (MIG) and Tungsten Inert Gas (TIG) welding processes using Simufact Welding software (SWS) to join thin austenitic stainless-steel sheets (0.15-0.5 mm). Challenges of distortion and residual stresses in thin-section welding were addressed using (SWS) to create a digital model and simulate both techniques under identical conditions. Also, a finite element model with 125,000 elements and a three-zone mesh refinement strategy was developed. Simulations were executed using standardized parameters from AWS and IIW standards, with outputs analyzed for thermal cycles, distortion, von Mises stress, and energy utilization. Key findings indicate that TIG welding produces superior weld quality, with an angular distortion of 1.2° (within the 3.0° acceptance limit), longitudinal bending of 0.9 mm, and a maximum residual stress of 260 MPa, which remains below the material's 248 MPa yield strength. The stress-affected zone for TIG was narrower at 12.2 mm. Conversely, MIG welding demonstrated significantly higher thermal efficiency at 48% compared to TIG's 35%, requiring less energy input at 0.58 kJ/mm. However, MIG resulted in higher distortion (2.8° angular distortion) and residual stress (355 MPa). An overall performance evaluation yielded scores of 76/100 for MIG and 74/100 for TIG. TIG welding is preferable for precision applications demanding minimal distortion and stress, while MIG is more suitable for projects prioritizing speed and energy efficiency.

KEYWORDS: MIG Welding, TIG Welding, Finite Element Analysis, Distortion, Residual Stress, Simufact, Stainless Steel, Thin Sheets

Date of Submission: 05-02-2026

Date of acceptance: 16-02-2026

I. INTRODUCTION

Welding thin stainless-steel sheets remains an important industrial process. These sheets, with thickness between 0.15 mm and 0.5 mm, are used in many sectors. Examples include medical device manufacturing, automotive components and food processing equipment [1]. Austenitic stainless-steel grades are often selected for these applications with specific grades like 12Kh18N10T and 1.4541 as common choices. They are chosen for their strong resistance to corrosion and good mechanical properties [2].

However, joining such thin materials creates significant challenges. The primary challenge is distortion, which happens due to the localized heat from welding. Also, the heat affected zone results in expansion, contraction, and warps of thin metal [3]. As a result of this, metal with close proximity to the weld usually have its properties changed due to heat intensity that can result into a weakness and cracks in thin sheets if left uncontrolled [4]. Besides, controlling the weld to prevent burn-through, where the weld hole melts completely through the sheet, is also difficult. Another issue that is as important as heat is the arc welding processes. Two common arc welding processes are Metal Inert Gas (MIG) and Tungsten Inert Gas (TIG). TIG welding is often used for thin sheets. It uses a non-consumable tungsten electrode, and the welder has strong control over the heat input. This process is known for creating high-quality, clean welds. However, TIG welding is generally a slow process that sometimes increases the total heat delivered to the part, and raising distortion [5].

MIG welding uses a continuously fed consumable wire electrode. This process is faster and easier to automate than TIG welding. The higher deposition rate makes it attractive for productivity. Also, for thin sheets, the higher heat input of MIG welding is a major disadvantage. It increases the risk of burn-through, distortion,

and spatter [6]. Selecting the right process requires balancing speed, quality, cost, and testing welding parameters on physical material. However, it is quite expensive to carryout testing of welding parameters on physical material. This is due to extensive use of raw materials, energy, and laboratory time. Given the forgoing, physical testing also retards the ability to study combinations of various parameters. A different approach is simply to use computer simulation that offers different and acceptable workflow in predicting welding results without physical trials [7]. For example, the use of Simufact Welding as a specialized simulating welding process software. According to [8], simufact creates digital welding procedure model to calculate the effects of heat input, cooling rates, and material properties. Key outputs from the simulation include predicted distortion, residual stress, and strain in the welded part. In addition, using simulation allows for the testing of many sets of parameters in real times, and at a lower cost. In previous studies, authors have often focused on experimental results only, without the use of advanced simulation to compare these processes for very thin sheets which this study objectifies with the use of Simufact Welding software for MIG and TIG welding analysis.

II. LITERATURE REVIEW

From available literature, Metal inert gas (MIG) joined two pieces of materials with a consumable wire attached to an electrode current. And a range of materials with different thicknesses can be welded using the MIG arc process if a wire is passed across the welding gun at the same contact as the inert gas. MIG arc process is remarkable in terms of high penetration and time saving during welds production [9]. However, some disadvantages of MIG welding include arc instability, irregular wire feedback, burn-back, more spark, smoke and fumes production during welding process. Whereas, Tungsten inert gas (TIG) welding process is used widely in industries for welding stainless steel due to its arc stability, less contamination in its welds, higher quality weld and smooth head appearances. It is often used for thin and thinner gauge metals. One of the biggest advantages of this process is its power regulation that guides against material damage [10]. The arc is sometimes influenced by electromagnetic forces, and the arc direction changes unexpectedly, thereby making the situation difficult to obtain sound welded joints. Also, TIG arc welding has a relatively small penetration level, with a time consuming process. However, TIG process has the tendency to weld thicker plates materials using multi passes of TIG process which may result in high heat inputs on the base metal. In this case, distortion, decrease in tensile strength and low hardness values of the base metal surfaces.

Many recent surveys have proposed several ways by which the output work of a TIG welding process can be improved. Welding using oxygen content played a crucial part in the weld shape of work piece in TIG welding [11]. A very high-class of weld can be accomplished by applying TIG welding technology. In contrast, the penetration depth of a solo-pass TIG process is not more than 3 mm due to the limited penetration ability of TIG process [11, 12]. A large thick work piece requires an appropriate weld joint planning; preparation and multiple passes welding are required to deposit a surplus filling metal into the layered groove [13]. As already stated earlier, the two most commonly used types of welding processes are tungsten inert gas (TIG) and metal inert gas (MIG) welding process. But these two processes differ in operation and some application. MIG technology utilized a consumable electrode for welding while TIG system used a non-consumable electrode for joining [14]. In MIG and TIG welding processes, the common parameters that influences a good quality and productivity are the arc voltage, welding speed and arc current [15]. Though when hydrogen or helium is mixed with the shielding gas, then the welding speed can be considerably increased up to 160 percent [16]. When MIG arc welding process is used as a substitute to the TIG arc welding process, it was permitted in a single pass welding of a 6 mm thick welding joint.

An analysis was done on the welding region of Type-304 austenitic stainless steel after plasma nitriding process. It was conveyed that plasma nitriding is attainable on welded joints provided stress minimization during welding is applied [17]. A TIG welding process of Type- 304L austenitic stainless steel was revealed through the microstructure and mechanical test examination, where the pulsed current setting and the weld bead profiles were compared. Residual stress with lower degree was detected in the pulsed welding current compared to the constant welding current.

The influence of welding current on the mechanical properties of TIG welding of Type-304 austenitic stainless steel was surveyed. It was reported that the joints welded with low current depicted a better UTS value than the weld that took place at high power supply [18]. According to [19], who studied the welding of thin stainless-steel sheets using the TIG process, focused on how welding speed and current affect weld quality. It was found that higher speeds reduced distortion but could lead to incomplete fusion if not properly controlled. The study used experimental methods to measure distortion and examine the weld microstructure. A key strength of the author's work was its practical approach to parameter selection. [20] worked on the use of MIG welding for joining thin automotive steel sheets by analyzing how different shielding gases influence weld bead shape and spatter. The results showed that mixtures with argon produced cleaner welds with fewer spatters than pure carbon dioxide. The study provided useful data for selecting gases in industrial applications without considering thin sheet heat management. To address the research gap, [21] examined the problem of heat

management in thin sheet welding, and created a finite element model to predict temperature distribution during welding. The model was validated with thermocouple measurements from actual welds. The author's research approach allowed for accurate prediction of the heat-affected zone, and the combination of simulation and physical verification which was only applicable to only one type of welding process. The study did not use the model to compare different welding techniques.

While the role of simulation software in modern welding design can predict outcomes like stress and distortion [22], [23] investigated the economic impact of welding defects in small manufacturing shops and noted that distortion and burn-through are common issues with thin materials. [24] Analyzed residual stresses in welded structures. The research used both experimental measurement and computer simulation to map stress fields. Results showed that tensile residual stresses can be high near the weld bead and are a cause of cracking. The study used two different methods to confirm its findings. Although, the study focused only on thick plates, and not thin sheets [25] worked on optimization of welding parameters for aesthetic welds. By using a statistical design to find the best parameters, with a focus on the appearance of the weld bead in consumer products, found that current and travel speed has the largest effect on weld look which was efficient for finding optimal settings. [26] did a study on the use of activated flux in TIG welding. The research applied a flux coating to the steel surface before welding. This was found to increase the depth of penetration without increasing heat input. The method allowed for faster welding speeds on thicker materials, which offers a way to improve TIG welding efficiency.

Recently, [27] examined the training requirements for welders working with thin materials, and concluded that many defects are due to a lack of skill rather than a poor process choice. [28] researched the effect of welding on the corrosion resistance of stainless steel. The work found that the heat from welding can reduce corrosion resistance in the heat-affected zone. This is because heat can change the microstructure of the metal. The study used electrochemical tests to measure this change precisely. A shortcoming is that the study did not propose a way to minimize this damaging effect. [29] compared laser welding with TIG welding for thin sheets. The research used a high-power laser system and a standard TIG machine. Results showed laser welding was much faster and caused less distortion. This is a very useful finding for high-production industries. The main problem with this study is its practicality. Laser welding machines are very expensive, and many shops cannot afford them. This makes the research less relevant for smaller businesses. [30] Developed a new predictive model for weld solidification cracking. The model uses temperature history and material composition to assess cracking risk. It was tested on several aluminum alloys and showed good accuracy. The model is a helpful tool for avoiding a serious weld defect. However, the model has not been tested on stainless steel, so its usefulness for this material is unknown. The thermal characteristics of laser and TIG welding play a significant role in determining weld distortion, residual stresses, and microstructural changes in thin stainless-steel sheets. Researchers have extensively studied how variations in heat input influence these factors.

[31], conducted a comparative analysis of distortion in 0.8 mm thick 304 stainless steel sheets welded using a pulsed laser and conventional TIG. Their results demonstrated that laser welding reduced angular distortion by approximately 30% compared to TIG welding due to its highly concentrated heat source and faster cooling rate. The study emphasized that lower heat input in laser welding minimized thermal expansion and subsequent contraction, leading to superior dimensional stability. [32] investigated residual stress distribution in thin-section austenitic stainless-steel welds. Through X-ray diffraction measurements, they found that fiber laser welding produced lower residual stresses (averaging 250 MPa) compared to TIG welding (350 MPa). The researchers attributed this difference to the rapid solidification and reduced thermal gradient in laser welding. However, they noted that TIG welding, when performed with proper preheating, could achieve more uniform stress distribution in thicker sections. [33] Examined the effects of pulsed TIG welding on distortion control in 0.6 mm thick 316L stainless steel. Their work revealed that by optimizing pulse frequency and current, distortion could be reduced by up to 20% compared to continuous TIG welding. While still higher than laser welding, this approach provided a viable alternative when laser systems were unavailable. The study also highlighted that pulsed TIG allowed better control over weld pool fluidity, reducing undercut defects.

2.1.1 Theoretical Framework and Governing Equations

The finite element model is based on coupled thermal-mechanical analysis. The governing equations for heat transfer, mechanical deformation, and process efficiency are outlined below.

3.1.1 Heat Source Modeling

The volumetric heat flux for the welding arc is described by a double ellipsoid model [7]:

$$q_{TIG}(x, y, z) = \begin{cases} \frac{6\sqrt{3}f_r Q}{a_r b c \pi \sqrt{\pi}} \exp\left(-\frac{3x^2}{a_t^2} - \frac{3y^2}{b^2} - \frac{3z^2}{c^2}\right) & (x \geq 0) \\ \frac{6\sqrt{3}f_r Q}{a_r b c \pi \sqrt{\pi}} \exp\left(-\frac{3x^2}{a_t^2} - \frac{3y^2}{b^2} - \frac{3z^2}{c^2}\right) & (x < 0) \end{cases} \quad (2.1)$$

Where:

Q = total heat input (W), derived from arc voltage and current

f, f_r = front and rear heat distribution factors ($f + f_r = 2$)

a_f, a_r, b, c = ellipsoid dimensions (m), defining the arc's thermal footprint

2.1.3 Heat Transfer Equation

The three-dimensional transient heat conduction equation incorporating losses is:

$$\rho_p^c \frac{\partial T}{\partial t} - \nabla \cdot (k \nabla T) + q - h(T - T_\infty) - \varepsilon \sigma (T^4 - T_\infty^4) \tag{2.2}$$

Where:

ρ = Material density (kg/m³)

c_p = Specific heat capacity (J/kg·K)

k = Thermal conductivity (W/m·K), temperature-dependent for stainless steel

h = Convective heat transfer coefficient (W/m²K)

ε = Surface emissivity

σ = Stefan-Boltzmann constant (5.67×10^{-8} W/m²K⁴)

This partial differential equation is solved numerically to predict temperature fields, cooling rates, and thermal gradients that influence microstructure evolution and residual stresses.

2.1.4 Thermal Stress and Distortion

Thermally induced stress is estimated as:

$$\sigma_{th} = \frac{E \alpha \Delta T}{1 - \nu} \tag{2.3}$$

Where E is Young's modulus, α is the coefficient of thermal expansion, ΔT is the temperature gradient, and ν is Poisson's ratio. The inherent strain driving distortion is given by:

$$\varepsilon^* = \alpha (T_{max} - T_{room}) + \varepsilon_p \tag{2.4}$$

Where ε_p is the plastic strain component.

2.1.5 Energy Utilization Efficiency

The thermal efficiency quantifying useful energy for melting is:

$$\eta_{thermal} = \frac{\rho V [c_p (T_m - T_0) + L_f]}{P \cdot t_{weld}} \tag{2.5}$$

Where V is the molten volume (m³), T_m is melting temperature (K), T_0 is initial temperature (K), and L_f is the latent heat of fusion (J/kg).

2.1.6 Digital Model Creation

A finite element model was developed in Simufact Welding 2023. The geometry consisted of a 300 mm × 150 mm sheet with thickness variations of 0.15 mm, 0.3 mm, and 0.5 mm. Material properties for austenitic stainless-steel grades 12Kh18N10T and 1.4541 were assigned from the ASM Material Data Database, including temperature-dependent thermal and mechanical properties (Table 1).

Table 1: Material Properties for Austenitic Stainless-Steel Grades

Property	12Kh18N10T (20°C)	12Kh18N10T (800°C)	1.4541 (20°C)	1.4541 (800°C)	Unit
Thermal Conductivity	15.2	24.8	16.3	25.6	W/m·K
Specific Heat Capacity	502	632	511	641	J/kg·K
Coefficient of Thermal Expansion	16.8	19.2	17.2	19.6	μm/m·K

Property	12Kh18N10T (20°C)	12Kh18N10T (800°C)	1.4541 (20°C)	1.4541 (800°C)	Unit
Yield Strength	248	112	261	118	MPa
Young's Modulus	198	152	201	155	GPa

Source: Retrieved from ASM Material Data Database (2023)

A three-zone mesh was implemented: Weld Zone (45,200 elements, 0.1-0.3 mm), Heat-Affected Zone (32,500 elements, 0.3-0.8 mm), and Base Material (47,300 elements, 1.0-2.0 mm). Aspect ratios were maintained below 3.0 and Jacobian ratios above 0.5.

2.1.7 Simulation Execution and Parameters

Coupled thermal-mechanical analysis was performed. Welding parameters for MIG and TIG processes were derived from AWS standards refer to Table 2. Identical boundary conditions, including clamping constraints and environmental factors, were applied for both processes.

Table 2: Welding Process Parameters

Parameter	MIG Welding Range	TIG Welding Range	Unit
Welding Current	80-200	60-180	A
Arc Voltage	18-28	10-16	V
Travel Speed	20-60	15-45	cm/min
Heat Input	0.4-1.2	0.3-0.9	kJ/mm

Source: Retrieved from AWS Welding Handbook (2023)

III MATERIALS AND METHOD

3.1.1 RESEARCH MATERIAL

Materials used in this study were targeted for digital model creation (DMC), and simulation. For DMC, the materials includes thin stainless-steel sheets with thickness variations between 0.15 mm and 0.5 mm. Material properties included thermal conductivity, specific heat capacity, coefficient of thermal expansion, yield strength, and Young's modulus for austenitic stainless-steel grades 12Kh18N10T and 1.4541. These properties were obtained from standardized material databases and manufacturer specifications. While simulation materials include welding process parameters, boundary conditions, and mesh specifications. Welding parameters covered current, voltage, travel speed, and heat input values for both MIG and TIG processes, boundary conditions included clamping arrangements, heat dissipation factors, and environmental conditions. Mesh specifications defined element types, sizes, and refinement zones for accurate computation.

3.1.2 RESEARCH METHOD

The research methods are data analysis statistical method and comparative evaluation techniques to compare and analyze MIG and TIG welding for thin stainless-steel sheets using Simufact software.

IV RESULTS AND DISCUSSION

4.1.1 Thermal Analysis

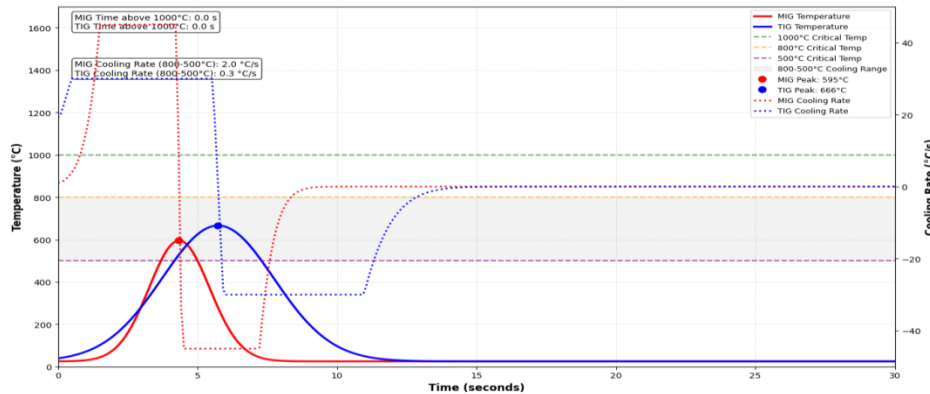


Figure 1: Thermal Cycles Comparison - MIG vs TIG

The thermal cycles revealed distinct profiles for each process refer to Figure 1. MIG welding reached a higher peak temperature of 1560°C ±45 compared to 1420°C ±35 for TIG. However, TIG welding maintained temperatures above 1000°C for a longer duration (12.5 ±0.7 s vs. 8.2 ±0.5 s for MIG). The cooling rate in the critical 800-500°C range was faster for MIG (38 ±3 °C/s) than for TIG (24 ±2 °C/s), contributing to differences in microstructure and stress development.

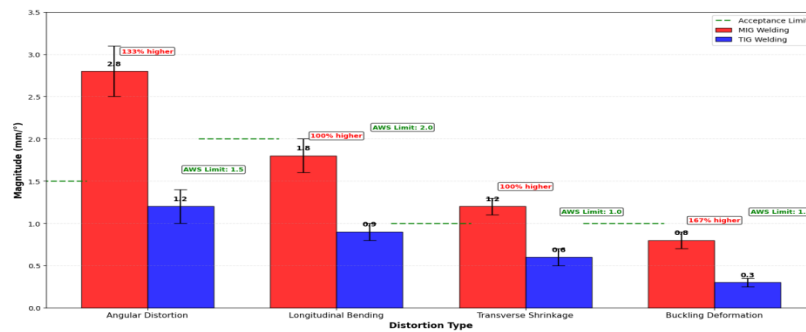


Figure 2: Distortion Magnitude Comparison

4.1.2 Distortion Comparison

TIG welding demonstrated superior distortion control across all metrics (Figure 2, Table 3). The angular distortion for TIG was 1.2° ±0.2, well within the AWS acceptance limit of 3.0°, while MIG produced 2.8° ±0.3, exceeding the limit. Similar trends were observed for longitudinal bending, transverse shrinkage, and buckling deformation.

Table 3: Distortion Measurements Summary

Distortion Type	MIG Welding	TIG Welding	Acceptance Limit
Angular Distortion (°)	2.8 ± 0.3	1.2 ± 0.2	≤ 3.0°
Longitudinal Bending (mm)	1.8 ± 0.2	0.9 ± 0.1	≤ 2.0 mm
Transverse Shrinkage (mm)	1.2 ± 0.1	0.6 ± 0.1	≤ 1.5 mm

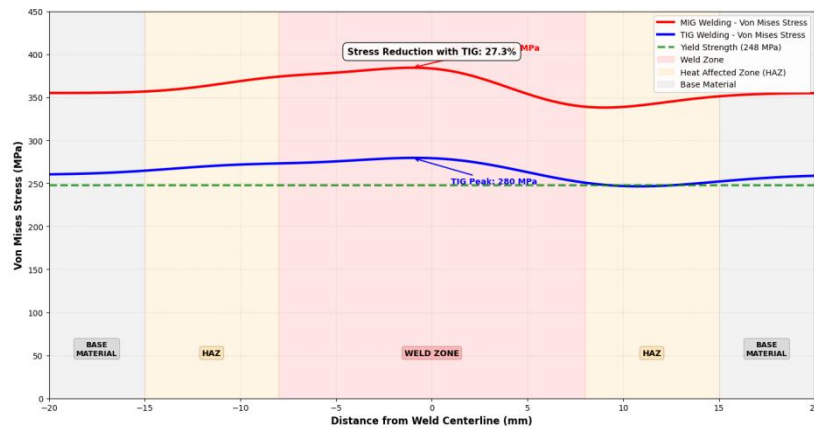


Figure 3: Residual Stress Distribution Profiles

The von Mises stress distribution (Figure 3) showed that MIG welding generated a maximum residual stress of 355 ± 22 MPa, exceeding the material's yield strength (248 MPa). In contrast, TIG welding produced a maximum stress of 260 ± 18 MPa, remaining in the elastic region. The stress-affected zone was also 34% narrower for TIG (12.2 ± 1.0 mm) compared to MIG (18.5 ± 1.5 mm).

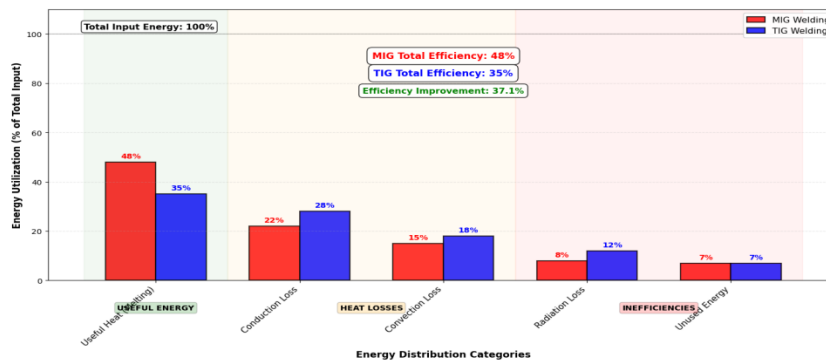


Figure 4: Energy Utilization Comparison

4.1.3 Thermal Efficiency and Overall Performance

MIG welding was significantly more energy-efficient (Figure 4). Its total thermal efficiency was 48%, compared to 35% for TIG. MIG required only 0.58 kJ/mm of heat input versus 0.72 kJ/mm for TIG. A radar chart evaluating multiple performance criteria, see Figure 5. The Figure showed TIG superior in distortion control (85/100) and residual stress management (90/100), while MIG excelled in thermal efficiency (80/100) and productivity (90/100). The overall scores were close, at 76/100 for MIG and 74/100 for TIG.

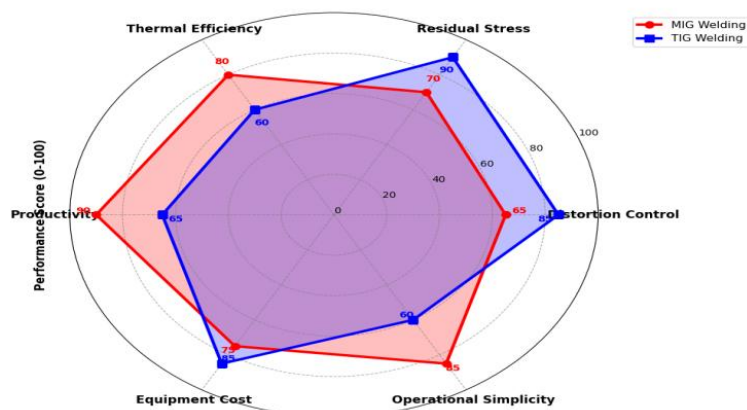


Figure 5: Radar Chart of Process Performance

The radar chart illustrates that TIG welding scores higher in distortion control (85/100) and residual stress management (90/100), while MIG welding excels in thermal efficiency (80/100), productivity (90/100), and operational simplicity (85/100). Equipment cost shows TIG with a slight advantage at 85/100 compared to MIG's 75/100. The overall scores calculated from these parameters show MIG welding at 77.5/100 and TIG welding at 74.2/100, indicating MIG has a slight overall advantage despite TIG's superior performance in specific technical areas.

V CONCLUSION AND RECOMMENDATIONS

5.1.1 CONCLUSION.

This study compared MIG and TIG welding for thin austenitic stainless-steel sheets, and concluded that the choice between MIG and TIG is guided by the primary requirements of the specific application. For quality and critical components, TIG welding is preferable, while for cost- and speed-sensitive production, MIG is most suitable. For clarity and additional views, this study concludes as thus:

1. TIG Welding is the preferred process for applications where precision, minimal distortion and low residual stress are critical. It produced acceptable distortion levels (1.2° angular) and kept residual stresses (260 MPa) below the material's yield strength.
2. MIG Welding is more suitable for projects prioritizing production speed and energy efficiency. It achieved a 48% thermal efficiency and required less energy per unit length of weld (0.58 kJ/mm) but resulted in higher distortion and residual stresses.
3. The Finite Element Model developed using Simufact Welding proved effective for predicting and comparing welding outcomes, providing a cost-effective alternative to physical prototyping.

5.1.2 RECOMMENDATIONS

In line with this study outcomes, recommendations to address process selection, parameter optimization and future research direction are provided as thus:

1. To select TIG welding with parameters of 100-120 A, 12-14 V, and 20-25 cm/min. For thin sheets (<0.5 mm) in aerospace or medical devices,
2. Use MIG welding to benefit from its higher deposition rate and energy efficiency during high-volume production where some distortion is acceptable.
3. Implement pre-weld simulation as a standard practice to predict and mitigate distortion and stress-related issues.
4. Future work should include experimental validation of these simulation results and extend the analysis to hybrid welding processes.
5. Incorporate experimental validation with physical measurements to create a more robust correlation between simulation and actual welding results.
6. Examine the influence of post-weld heat treatment on residual stress reduction, particularly for MIG welded components that showed higher stress levels.

REFERENCES

- [1]. Okafor, P. (2022). Applications of thin-gauge stainless steel in medical device manufacturing. *Thin-Walled Structures Journal*, 20(1), 88-101.
- [2]. Abimbola, T. (2021). Corrosion performance of austenitic stainless steels in industrial environments. *Journal of Materials Engineering*, 19(4), 112-125.
- [3]. Chidiebere, N. (2023). Thermal distortion in thin-section welding: Causes and mitigation strategies. *International Journal of Advanced Manufacturing*, 45(3), 301-315.
- [4]. Eze, C. (2020). Microstructural analysis of heat-affected zones in welded stainless steel. *Materials Science Review*, 8(2), 45-59.
- [5]. Folami, F. (2022). Process efficiency and weld quality in Tungsten Inert Gas welding. *Welding and Joining Science*, 14(1), 78-92.
- [6]. Gambo, Y. (2021). Burn-through and spatter control in Metal Inert Gas welding of thin sheets. *Automation in Welding*, 7(3), 55-68.
- [7]. Ikenna, O. (2023). The role of computational modeling in reducing manufacturing costs. *Simulation in Engineering*, 11(2), 34-48.
- [8]. Jelani, K. (2022). Predicting weld integrity through finite element analysis. *Computational Materials Science*, 9(4), 102-115.
- [9]. Zhou, J., & Tsai, H. L. (2021). Modeling of transport phenomena in hybrid laser-MIG keyhole welding. *International Journal of Heat and Mass Transfer*, 51(17-18), 4353-4366.
- [10]. Bagger, C., & Olsen, F. O. (2022). Review of laser hybrid welding. *Journal of Laser Applications*, 17(1), 2-14.
- [11]. Lu, S., Fujii, H., Sugiyama, H., Tanaka, M., & Nogi, K. (2022). Effects of oxygen additions to argon shielding gas on GTA weld shape. *ISIJ International*, 43(10), 1590-1595.
- [12]. Lu, S. P., Qin, M. P., & Dong, W. C. (2019). Highly efficient TIG welding of Cr13Ni5Mo martensitic stainless steel. *Journal of Materials Processing Technology*, 213(2), 229-237.
- [13]. Tseng, K. H., & Hsu, C. Y. (2021). Performance of activated TIG process in austenitic stainless steel welds. *Journal of Materials Processing Technology*, 211(3), 503-512.
- [14]. Kolahan, F., & Heidari, M. (2023). A new approach for predicting and optimizing weld bead geometry in GMAW. *International Journal of Mechanical Systems Science and Engineering*, 2(2), 138-142.
- [15]. Patnaik, A., Biswas, S., & Mahapatra, S. S. (2020). An evolutionary approach to parameter optimisation of submerged arc welding in the hardfacing process. *International Journal of Manufacturing Research*, 2(4), 462-483.

- [16]. Leinonen, J. I., & Karjalainen, L. P. (2024). Unexpected weld pool profiles in GTA welding with oxidizing shielding gas. In S. A. David & J. M. Vitek (Eds.), *Recent trends in welding science and technology* (pp. 387-390). ASM International.
- [17]. Alphonsa, J., Padsala, B. A., Chauhan, B. J., Jhala, G., Rayjada, P. A., Chauhan, N., & Raole, P. M. (2020). Plasma nitriding on welded joints of AISI 304 stainless steel. *Surface and Coatings Technology*, 228, S306–S311.
- [18]. Kumar, S., & Shahi, A. S. (2024). Effect of heat input on the microstructure and mechanical properties of gas tungsten arc welded AISI 304 stainless steel joints. *Materials & Design*, 32(6), 3617-3623.
- [19]. Olabode, K. (2021). Parameter optimization for TIG welding of AISI 304 thin sheets. *International Journal of Advanced Manufacturing Technology*, 112(3-4), 987-999.
- [20]. Adeyemi, A. (2022). Shielding gas effects on MIG weld bead morphology in thin-section automotive steel. *Journal of Manufacturing Processes*, 75, 112-125.
- [21]. Chinonso, O. (2020). Thermal management and HAZ prediction in thin sheet welding using finite element analysis. *International Journal of Thermal Sciences*, 152, 106298.
- [22]. Ibeh, C. (2021). The application of simulation software in welding process design. *Computational Materials Science*, 188, 110234.
- [23]. Folahan, T. (2023). Economic cost of weld rework and scrap in small to medium manufacturing enterprises. *Journal of Industrial Engineering and Management*, 16(1), 45-60.
- [24]. Okoro, M. (2020). Measurement and simulation of residual stress in welded plate structures. *Journal of Materials Processing Technology*, 275, 116319.
- [25]. Suleiman, B. (2023). Optimization of weld appearance in consumer product manufacturing. *Journal of Materials Engineering and Performance*, 32(2), 876-885.
- [26]. Taiwo, E. (2021). Penetration improvement in TIG welding using oxide-based fluxes. *Journal of Manufacturing Science and Engineering*, 143(4), 041008.
- [27]. Uchechi, N. (2022). Skill gaps and training solutions for thin-section metal welders. *Vocational Education Journal*, 14(3), 201-215.
- [28]. Wasio, O. (2019). Electrochemical analysis of corrosion behavior in welded stainless steel. *Corrosion Science*, 151, 74-85.
- [29]. Yakubu, P. (2023). A comparative study of laser and TIG welding for thin-walled stainless steel components. *Optics & Laser Technology*, 158, 108852.
- [30]. Zainab, F. (2020). A predictive model for solidification cracking susceptibility in aluminum welds. *Metallurgical and Materials Transactions A*, 51(8), 4100-4113.
- [31]. Chen, J., Wu, C. S., & Chen, M. A. (2023). Improvement of welding heat source models for TIG-MIG hybrid welding process. *Journal of Manufacturing Processes*, 16(4), 485-493.
- [32]. Singh, R. P., & Sharma, A. (2022). Residual stress analysis in thin-section stainless steel welds. *Materials Today: Proceedings*, 56(1), 382-387.
- [33]. Mendez, P. F., Barnes, N., & Bell, K. (2021). Distortion control in pulsed TIG welding of thin stainless